Thermal and Structural Properties of Succinite Reinforced PA6 Nanofibers

Inga Lasenko
JLU Technologies Ltd
(of Affiliation)
Riga, Latvia
info@jlutechnologies.com

Abstract. **Give This research article delves into the thermal stability of succinite -an organic polymer- when amalgamated within the structure of PA6 nanofibers, with a focus on assessing the consequent mechanical and structural performance of such composite nanofibers. The electrospinning method employed, involves the process of heating and high voltage to polymers, is known to inherently alter their thermal properties. The primary objective of this study is to examine the thermal stability of succinite within the PA6 nanofiber matrix and to evaluate the preservation of the composite material's mechanical and structural integrity, particularly under varying PA6 concentrations (16%, 20%, and 28%). Through thermal analysis techniques such as Differential Scanning Calorimetry (DSC), Thermogravimetric Analysis (TGA), and Infrared (IR) spectroscopy, it was observed that the succinite nano powder (ranging from 5-20 nm) exhibits minimal loss of volatile components, notably the NH amino group, upon heating to 150 ºC—a common solvent temperature during suspension preparation. This loss does not surpass 0.1% of the original volume, ensuring the predominance of critical components like succinite acid ($C_4H_6O_4$) in the composite. Furthermore, PA6 nanofibers were fabricated with varying PA6 polymer percentages (16%, 20%, and 28%) and with or without the integration of succinite nano powder, to compare mechanical properties. It was noted that incorporating succinite into PA6 nanofibers (at 16% concentration) led to an increase in fibre diameter to 78±14 nm from the 60±17 nm diameter of pure PA6 fibres, alongside a notable decrease in elastic modulus by approximately 2.3 times. However, the ultimate tensile strength only marginally reduced from 295.2 MPa to 274.9 MPa, with a slight decrease in toughness from 168.3 to 162 MPa. Contrary to pure PA6 fibres, the strain-to-failure ratio for the composite nanofibers saw an approximate 7% increase. This study elucidates the subtle yet significant modifications in the mechanical and structural properties of polymer composites attributable to their thermal stability. These findings furnish vital insights for the application of such composite materials in diverse thermal management contexts, particularly when utilised as protective materials.**

Keywords: PA6 (Polyamide 6), Nanofibers, Electrospinning, thermal analysis, Nylon 6.

I. INTRODUCTION

This Over the years, there has been a dramatic increase in the manufacturing of composite nanomaterials (based on the electrospinning process) for many applications such as aerospace, automobile, electronic packaging, food packaging, medical, etc., included an innovative recycled technologies of these materials [1], [2], [11]–[15], [3]–[10]. To overcome existing limitations in new material design, scientists paying attention to new approaches [16]–[19] , ways of 3D printing [20]–[22], material combinations [23]–[25] and nanoparticle use in a newly studied class of composites a syntactic foam [26]. Using organic, inorganic, and their combinations fillers has become widespread in polymeric systems [27], [28] . The purpose of adding synthetic or natural inorganic fillers to the polymer matrix is to improve composite properties and subsequently reduce production costs [29]. Furthermore, the presence of nanoparticles that act as reinforcement fillers can affect changes in the polymer matrix in terms of flowability, viscosity, colour, density, and subsequently also tends to improve the optical, electrical, catalytic, magnetic, mechanical, and thermal properties of the composite nanomaterials [30].

The last indicator is very important for determining the thermal characteristics of the polymer structure, which has a decisive impact on the mechanical parameters of the composite polymer as a whole.

Assessing the most widely used polymers (as a material with protective properties), it is necessary to note PA6 [31], on which we focus in this work. As fillers (to obtain a composite polymer), a natural organic polymer is used - succinite, the protective effects of which (mainly is UV protection in an absorbance peak (0.75) at wavelength 244 nm) are quite well covered in scientific publications. Furthermore, succinite is a biologically active element, and the smaller particle size (diam.<20 nm), the higher the activity of succinite, due to the presence of pure succinic acid and succinic acid salts in its structure [32].

The structure of polyamide 6 reinforced with succinite is known, but not enough is described in scientific works.

Print ISSN 1691-5402
Online ISSN 2256-070X
https://doi.org/10.17770/etr2024vol3.8149

The difficulty in analyzing the structure of a nanomaterial with succinite inclusions lies that the succinite particles are very heterogeneous and have a size of up to 1-3 microns, besides, in most cases described, the succinite particles are entangled in nanofibers and are not part of their structure [33].

In this study, a new PA6 composite nanofibres with integrated succinite particles in their structure were received and studied. For this purpose, we used specially processed amber powder obtained by fine grinding protocols [34], particle size 5-20 nm (obtained from the company JLU Technologies, Riga, Latvia). Using finely ground succinite powder, by electrospinning process homogeneous composite nanofibers were obtained, and this method has proven itself well, which made it possible to carry out all the necessary tests in full.

It is well-known that the thermal properties of the succinite material come from its structure and polymer composition. The main structural elements of succinite are compounds of aromatic and hydroaromatic sequences with condensed nuclei consisting of conjugated double bonds of carboxylic, hydroxyl, and ester groups. Succinite is essentially characterised by a three-dimensional structure with a rare lacing destroyed by heating and the mechanical effect due to the cleavage of chemical bonds, which implies the formation of free radicals.

Therefore, the composite nanomaterial (under mechanical and thermal treatment in the time of its processing) should retain all its mechanical and structural (biological) properties. To achieve this, the thermal properties of succinite (Baltic Amber) must be researched.

The aim of this article is to study the thermal stability of succinite (organic polymer) that is integrated into the PA6 nanofiber structure, and with this, it is necessary to estimate how the composite polymer materials (with variation of PA6 concentration of 16%, 20%, and 28%) retain its mechanical and structural (biological) properties.

II. MATERIAL AND METHODOLOGY

This study meticulously examined the thermal characteristics of succinite particles in electrospun PA6 nanofibers. For a more detailed comparative thermal study, the succinite particles were studied separately (Amber Raw and Amber Raw Powder were examined). And the second part of the work was estimated how the composite polymer materials (with variation of PA6 16%, 20%, and 28% concentration) retain their mechanical and structural (biological) properties. The composite nanofibres were produced (by electrospinning method) like described in our previous work [8].

This new composite nanomaterial consists of a polymer matrix, which is Polyamide 6 (NYLON 6), type RADIPOL S100-004® with a low molecular content of 0.9% and a melting temperature of 220 °C, received from Sigma-Aldrich AB, Germany. The fillers are succinite powder (CAS: 9000-02-6; EC: 232-520-0) with a particle size (5-20 nm, d98%<20 nm), the source (Baltic amber) contains about 8÷12% succinic acid, received from JLU Technologies Ltd, Riga, Latvia.

To illustrate the difference of thermal parameters between the Amber Raw Powder (5-20 nm) and Amber Raw (<5 mm), were conducted their comparative thermal analysis.

Thermal analysis include:

a) Thermogravimetric analysis (TGA) (testing according to ISO 11358) is a thermal analysis technique which consists of measuring the variation in mass of sample as a function of time, for a given temperature or temperature profile.

Thermogravimetric tests of the succinite samples were performed on a NETZSCH TG 209 F1 Iris instrument (Germany). The sample mass is 17.0963 mg (Amber Raw, not treated), 6.3284 mg (Amber Raw Powder) were heated in nitrogen at 450 °C. The thermal stability of the succinite material was evaluated from the weight loss heating curves. The thermal degradation temperature was calculated using the original NETZSCH PROTEUS software.

b) Differential scanning calorimetry (DSC) is a thermal analysis technique. Measures the differences in heat exchange between samples to be analysed and referenced.

The DSC tests (testing according to ISO 11357) of the succinite samples were performed on a NETZSCH differential scanning calorimetry (DSC) 204 F1 Phoenix instrument (Germany). The sample mass is 19.8808 mg (Amber Raw, particles ø <5 mm), 4.1922 mg (Amber Raw Powder, ø <20 nm) by weight, using nitrogen as the purge gas with a flow rate of 20 ml/min in the temperature range of 25 to 450 °C. The heating was operated at a rate of 20 °C/10 min. The glass transition temperature Tg was calculated from the experimental heating curve.

Fourier transform infrared spectroscopy (FTIR, testing according to ISO 19702:2015(En)) is a common method for determining the chemical composition of succinite. The FTIR spectra were recorded on a Varian Scimitar 800 FT-IR spectrometer (Germany).

To perform a comparative analysis of the chemical composition, succinite samples were studied without thermal pretreatment and after heating, as indicated in Table 1.

TABLE 1 CRYSTAL SIZE OF EACH CRYSTAL PHASE FOR WELL-ALIGNED COMPOSITE NANOFIBERS WITH AVERAGE DIAMETERS OF 50, 90 AND 340 NM.

No. of sample	Type of Baltic Amber	Condition of preparation
1	succinite	Without preheating, standard;
2	succinite	Heated to 150.0 ºC in the drying chamber; the chamber was vacuumed to 10^{-1} mmHg.

The samples were preheated using the Memmert UFB 500 universal drying oven (Germany); range 30-250 ºC; exactitude: for the chosen temperature 0.5 °C, for the factual temperature – 0.1 ºC (<99.9 ºC) and 0.5 ºC (>100 ºC) – for the keeping of samples at the temperature of 150 °C, continue 10 min.

The test material was succinite (Amber Raw Powder), the weight of the sample was 3.8 mg. For weighing of samples, analytical balance KERN PCB M was used (KERN&Sohn GmbH; D-72336, Balingen, Germany;

accuracy class: II high, max up to 200 g, discreteness 0.01 g; calibration certificate number: M0901K23, 15.06.2023).

To obtain a succinite tablet, succinite was initially reduced for 15 minutes to a fine particle in the Retsch® MM200 ball mill (powerful impact and friction, up to 25 Hz) (Retsch GmbH, 42781 Haan, Rheinische Str.36, Germany), after which the raw Amber Raw Powder was mixed with 361 mg of KBr powder. The tablet was obtained by pressing the mixture of succinite powders and KBr (CAS No. 7758-02-3) (received from Sigma-Aldrich chemicals, Merck KGaA, Darmstadt, (64287) Germany), which was placed on the spectrometer. The measurement range was 400-4000 cm^{1} and an accuracy of ±4 cm^{-1} using KBr as beam splitter.

III. Results and Discussion

In order to study the properties of succinite, thermal analysis methods were applied. These methods are applied to the search for chemical reactions, phase, and other physic-chemical transformations occurring under the influence of heat in chemical compounds. Thermal processes are accompanied by an alteration of internal heat-endothermic and exothermic transformations. These thermal effects can be discovered using thermogravimetric analysis (TGA) and differential scanning calorimetry (DSC) methods, which determine the quantitative heating effects occurring in the sample material.

A. Thermogravimetric analysis (TGA)

The curve shows (Fig.1) the thermal decomposition of Amber Raw (before grinding), according to the TGA curve, noting that the thermal decomposition of the succinite takes place in two stages: the first decomposition at an onset temperature (382.3 °C) with a mass loss of 23.5% and the second decomposition at an infection temperature (384.8 °C) linked to a chemical reaction which leads to a mass loss of 15.17%.

In this thermal analysis, a mass loss of 38.67% was recorded for the Amber Raw in a temperature range between 25 °C and 400 °C.

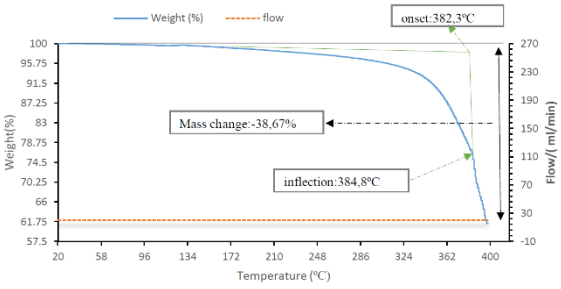

Fig. 1. TGA thermogram of Amber Raw (mass (%) as a function of temperature (ºC)).

Fig. 2 presents the TGA curve of Amber Raw Powder (after grinding); according to this curve, a mass loss of 100% has been recorded for Amber Raw Powder with an onset temperature of 417.9 °C and an inflection temperature of 420.4 °C after 8 min. of heating. The total decomposition of Amber Raw Powder has been recorded.

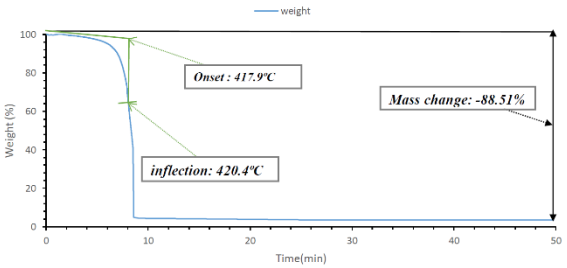

Fig. 2. TGA thermogram of the raw amber powder (mass (%) as a function of time (min.)).

By comparing the results in the two cases Amber Raw and Amber Raw Powder a difference in the thermal decomposition is around 38 °C; in the case of Amber Raw the thermal decomposition started at a temperature of 382.3 °C, on the other hand, of Amber Raw Powder the sample remains stable up to a temperature of 420.4 °C at the level of mass loss for Amber Raw Powder, there is a total decomposition; on the other hand, in the case of Amber Raw (before grinding) the mass loss does not exceed 40%.

B. Differential Scanning Calorimetry (DSC)

Fig. 3 shows the DSC diagram for Amber Raw. We can observe the presence of an exothermic peak with a ΔH=35.16 J/g, this peak is due to a glass transition at the sum of the peak, we observe an intersection with the shape of the DSC curve at a temperature of 136.3 °C, this temperature is corresponding the glass transition temperature.

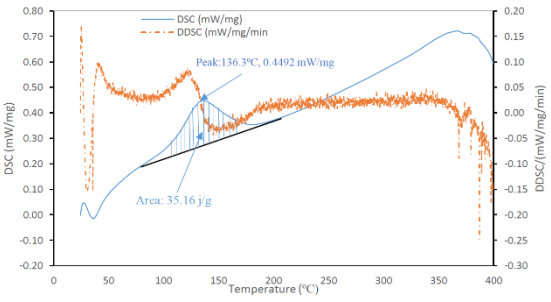

Fig. 3. DSC thermogram of Amber Raw (DSC (mW/mg) as a function of temperature (ºC)).

In Fig. 4 presents the diagram DSC in the case of Amber Raw Powder in a temperature range between 25 °C and 400 °C according to the curve by noting the presence of two peaks: an exothermic peak linked to the transition glassy, and a second endothermic peak linked to melting at temperatures of 136 °C and 263 °C, respectively.

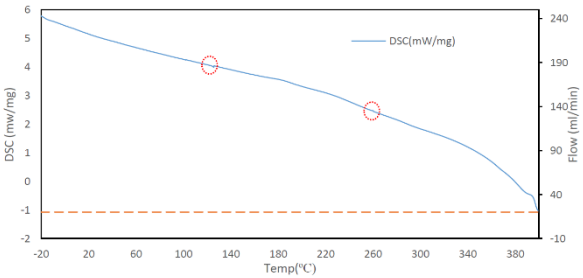

Fig. 4. DSC thermogram of Amber Raw Powder (DSC (mW/mg) as a function of temperature (ºC)).

C. Method of determination of chemical composition

In order to study the chemical composition of the sample (Amber Raw Powder), spectral analysis was carried out. 15 samples were taken, and the mean spectral curve was shown (Fig. 5; 6).

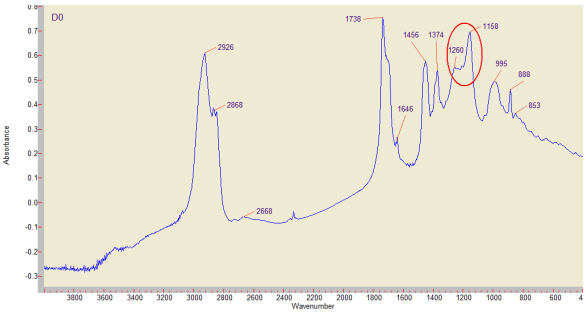

Fig. 5. FTIR spectrum of Amber Raw Powder (< 20 nm), 0 min).

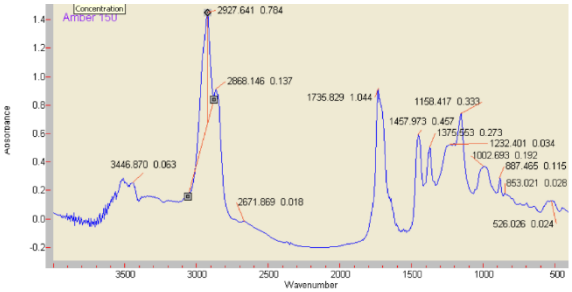

Fig. 6. DSC FTIR spectrum of the Amber Raw Powder (< 20 nm), 10 min, heated up to 150.0 ºC

According to the "Table of discriminating frequencies in the IR spectrum of atomic groups" [35], the following elements have been determined: the absorption band 850-1000 cm^{-1} proves the presence of peroxides; 950-1200 cm^{-1} - cyclic ethers; 1105-1360 cm^{-1} - phenol hydroxides; 1420-1450 cm^{-1} - distorting oscillation of the 2 groups; 1575-1630 cm^{-1} - polycyclic aromatic compounds; 2800-3100 cm^{-1} - carboxylic groups; 3300-3500 cm^{-1} - NH amine groups. By comparing the results of the spectral analysis of succinct samples (Fig. 5; 6), it can be seen that the difference in the alteration of the values of the frequencies characteristic of the atomic groups of the polymer constitutes the maximum of 0.005 %. The greatest changes in the value of the characteristic frequencies of the atomic groups (Fig. 5; 6) correspond to the change in the value of the NH amine group representing 0.1% (the value of succinite without preheating, standard).

In the samples of raw amber powder, the "horizontal shoulder" was observed; it is characteristic to the Baltic amber at 1180-1240 cm^{-1}, which indicates that it contains succinic acid ($C_4H_6O_4$). Furthermore, when exposed to a temperature of 150.0 °C, it does not cause changes in the structure of the “horizontal shoulder” (Fig. 6), which correlates with references to thermal and structural studies of Baltic amber [36].

D. Determination of the mechanical characteristic of nanofibers with/without the succinite particles

To determine the change of the mechanical parameters in polymer materials (with variation of PA6 16%, 20% and 28% concentration), as well with/without succinite, taking into account its heat treatment, an analysis of the mechanical characteristics of nanofibers was carried out (Fig. 7).

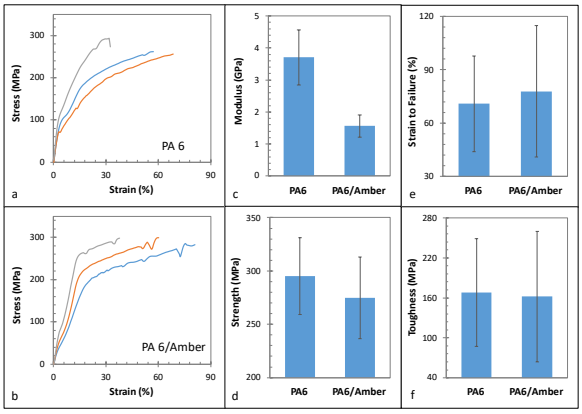

Fig. 7. The Stress as a function of strain for (a) nanofibres (curves: grey color: PA6 28%, average $diam_{nanofiber}$ = 230±15 nm; curve: blue colour: PA6 20%, average $diam_{nanofiber}$ = 150±19 nm; curve: red colour: PA6 16%, average $diam_{nanofiber}$ = 60±17 nm); (b) composite nano fibres (with succinite powder 5-20 nm) (curves: grey colour: PA6 28%, average $diam_{nanofiber}$ = 239±11 nm; curve: blue colour: PA6 20%, mean $diam_{nanofiber}$ = 166±18 nm; curve: red colour: PA6 16%, average $diam_{nanofiber}$ = 78±14 nm); (c) elastic modulus (GPa) of nanofibers with/without the succinite powder; (d) tensile strength (MPa) of nanofibers with/without the succinite powder; (e) strain to Failure (%) of nanofibers with / without succinite powder; (f) Toughness (MPa) of nanofibers with/without the succinite powder.

According to Fig. 7-a, the maximum value of the stress for the polymer (28%) has a value at 294±9 MPa after there is a break at a deformation of 31.75%. The stress values between 20% and 16% are different only on 10.2 MPa. The stress value of the polymer (16%) at 255±13 MPa, the value of deformation at break can go up to 68.33%. Fig. 7-b show the stress values as a function of strain for the composite nanofibers (with succinite powder). According to this figure, there is not a remarkable increase in stress values because the maximum values (PA 28%, the same for PA 16%) are around 299±14 MPa, but with this constraint the rupture manifests itself at a deformation value, which went up to 60% (PA 16%), but for PA 28% less (42%). The curve (PA 20%) that the strain at break can increase to a value of 81% with a stress value of 283±10 MPa, while this is not the case in the pure polymer (polyamide without succinite powder).

In general, when comparing the stress values of polymers (16%, 20%, 28%) with/without succinite powder, a progressive decrease in the stress values as for polyamide with succinite powder from 299±14 MPa till 283±10 MPa, as for pure polyamide from 294±9 MPa till 256±13 MPa. The difference in stress characteristics between PA6 with/without succinite powder is approximately 44 MPa (higher border (299±14 MPa) and lower border of stress values (256±13 MPa). This can be explained by the presence of succinite nanoparticles (5-20 nm) in the structure of nanofibers, as an element that weakens the stress of the cross section in the nanofiber, as well as a decrease in the average diameter of the nanofibers (from 230±15 nm till 60±17 nm). These observations correlate well with the references [37]. However, more non-linear behaviour of the stress-strain characteristics was observed for PA6 without succinite powder, against the stress-strain characteristics of PA6 with succinite powder, which have more classic elastic-plastic behaviour.

The effect of heat treatment (for both types of polymers) was manifested in the example of PA6 (16%) with succinite powder (nanofiber diameter 78±14 nm). At high stress value, about 299±14 MPa composite showed almost 21% less strain compared to PA6 (20%) with succinite powder (nanofiber diameter 166±18 nm). This behaviour can be explained by the crystalline orientation of molecules in polymers of nanofibers with succinct particles (this was obtained based on the basis of XRD and Raman tests and described in our next studies).

Figs. 7-c show the average Elastic Modulus values for the two types of samples (PA6 with a concentration of PA6 16%, 20%, 28% and with/without the succinite powder). For PA6 only the modulus reaches a value of 3.7 GPa but this value remains within a range of values 2.9-4.6 GPa; in the case of composite polymers, the elastic modulus has a lower value than of pure polymer, and due to increase in strain for the composite nanofibers with a very reliable change in the level of the stress which will return the value of the modulus lower this can be concluded from Equation (1), which linked the Modulus according to the stress and the strain.

$$Modulus = stress / strain \qquad (1)$$

Fig. 7-d shows the Strength values for the two types of samples (PA6 with PA6 concentration of PA6 16%, 20%, 28%, and with/without the succinite powder); and always as in the case of the Elastic Modules the values of the Strength for PA6 are higher on 20 MPa than Strength value of the composite polymer. The Strength value reaches 295.2 MPa and 274.9 MPa for both types of polymers, respectively. Changes of the Strength values in the data scatter limit are statistically "not significant".

Fig. 7-e presents a very important parameter, the Strain to Failure and according to the figure noting that on the other parameters the Modulus and the Strength which has a greater value for PA6 the Strain to Failure reach the greatest value in the case of composite polymer (77.8%), whereas for PA6 the value is only 70.9%. These changes can be demonstrated from Fig. 7-b in which we note that the strain values increase in a remarkable way with the increases the stress values, this may be linked to the increase in physical and chemical interactions between the PA6 matrix and succinite nano particles.

Fig. 7-f shows the toughness for the two types of samples. In this case, there is not a great difference between the two types of samples; there the Toughness values reach 168.3 and 162 MPa for both types of polymers, respectively.

The results presented in this study offer insightful contributions to the understanding of the thermal and mechanical properties of succinite-incorporated PA6 nanofibers. Thermal analysis through TGA and DSC methods has elucidated the distinct thermal decomposition and glass transition behaviours of Amber Raw and Amber Raw Powder, highlighting the impact of physical form on thermal stability. The observed increase in onset and inflection temperatures for Amber Raw Powder suggests that grinding the succinite into a powder form enhances its thermal stability, potentially due to an increase in surface area and more uniform heat distribution during analysis.

The mechanical analysis of nanofibers with varying concentrations of PA6 and the incorporation of succinite nanoparticles reveals nuanced alterations in stress-strain behaviour, elastic modulus, tensile strength, strain to failure, and toughness. The incorporation of succinite nanoparticles not only affects the diameter of the nanofibers but also modulates their mechanical properties. A notable observation is the reduction in the elastic modulus in composite fibres, which may be attributed to the dispersion of succinite particles within the PA6 matrix, potentially acting as stress concentrators or modifiers of the polymer chain mobility. This decrease in modulus, however, comes with an increase in strain to failure, suggesting enhanced ductility in the composite nanofibers. Such behaviour might be advantageous in applications requiring materials that can absorb more energy before failure, such as in impact-resistant coatings or flexible electronic components.

Furthermore, the slight decrease in tensile strength and toughness in composite fibres, while statistically not significant, points to a complex interplay between the reinforcing effect of the succinite particles and their impact on the polymer matrix's continuity. The observed mechanical behaviours underscore the importance of optimizing nanoparticle dispersion and polymer-nanoparticle interactions to achieve desired material properties.

IV. Conclusion

In accordance with the thermal analyses of the succinite nano powder (DSC, TGA and IR spectra) presented, it has been determined that the insignificant loss of volatile components, in particular the NH amino group, in the case of heating of succinite to 150 ºC (solvent temperature in time of suspension preparation) does not exceed 0,1% (of the original volume), hence the percentage of a relevant component such as the succinite acid ($C_4H_6O_4$) remains almost entirely in succinite.

Taking into account the results of thermal analysis of polymers, a comparative analysis of the mechanical parameters of PA6 nanofibers with/without succinite nano powder was carried out. As a result, it was established that the mechanical properties are close enough between the pure PA6 and composite nanofibers.

Determined that increasing the composite nanofiber (PA6 16% with nonstandard mechanical behaviour) diameter until 78±14 nm, in compare with pure PA6 nanofiber same concentration (with diameter 60±17 nm) resulted in simultaneous reduced in elastic modulus almost in 2.3 time, but a real strength decreased very slightly from 295.2 MPa to 274.9 MPa. A similarly minor change observed for toughness from 168.3 to 162 MPa. As opposed to pure PA6 nanofiber, the Strain to Failure value for the composite nanofiber was increased almost on 7%.

Despite the insignificant lower strength of the composite nanofiber in comparison to the PA6 nanofiber (without additives) the tensile properties of the composite nanofiber decreased about 2–2.8 times in comparison to initial the PA6 nanofiber. Nevertheless, the achieved strength of the composite nanofiber is enough to prepare the textile fabrics with protection properties because it is

used in combination with other natural and synthetic macrofibres.

ACKNOWLEDGEMENT

This work was supported by the European Union Horizon 2020 program ERA-NET Cofound M-era.Net 3; Project 3DNano-HPC, ES RTD/2022/13, LZP, 01.05.2022-30.04.2025.

REFERENCES

[1] A. Hussain, D. Goljandin, V. Podgursky, M. M. Abbas, and I. Krasnou, "Experimental mechanics analysis of recycled polypropylene-cotton composites for commercial applications," *Adv. Ind. Eng. Polym. Res.*, vol. 6, no. 3, pp. 226–238, 2023, doi: 10.1016/j.aiepr.2022.11.001.

[2] A. Hussain, V. Podgursky, M. Viljus, and M. R. Awan, "The role of paradigms and technical strategies for implementation of the circular economy in the polymer and composite recycling industries," *Adv. Ind. Eng. Polym. Res.*, vol. 6, no. 1, pp. 1–12, 2023, doi: 10.1016/j.aiepr.2022.10.001.

[3] A. Hussain, V. Podgursky, D. Goljandin, M. Antonov, F. Sergejev, and I. Krasnou, "Circular Production, Designing, and Mechanical Testing of Polypropylene-Based Reinforced Composite Materials: Statistical Analysis for Potential Automotive and Nuclear Applications," *Polymers (Basel).*, vol. 15, no. 16, 2023, doi: 10.3390/polym15163410.

[4] I. Lasenko, D. Grauda, D. Butkauskas, J. V. Sanchaniya, A. Viluma-Gudmona, and V. Lusis, "Testing the Physical and Mechanical Properties of Polyacrylonitrile Nanofibers Reinforced with Succinite and Silicon Dioxide Nanoparticles," *Textiles*, vol. 2, no. 1, pp. 162–173, 2022, doi: 10.3390/textiles2010009.

[5] A. Viluma-Gudmona, I. Lasenko, J. V. Sanchaniya, and B. Abdelhadi, "The amber nano fibers development prospects to expand the capabilites of textile 3D printing in the general process of fabrication methods," *Eng. Rural Dev.*, vol. 20, pp. 248–257, 2021, doi: 10.22616/ERDev.2021.20.TF051.

[6] D. Grauda, L. Bumbure, I. Lyashenko, A. Katashev, Y. Dekhtyar, and I. Rashal, "Amber particles as living plant cell markers in flow cytometry," *Proc. Latv. Acad. Sci. Sect. B Nat. Exact, Appl. Sci.*, vol. 69, no. 3, pp. 77–81, 2015, doi: 10.1515/prolas-2015-0011.

[7] A. Viluma-Gudmona, I. Lasenko, J. V. Sanchaniya, and A. Podgornovs, "Electro-resistant biotextile development based on fiber reinforcement with nano particles," *Eng. Rural Dev.*, vol. 20, pp. 804–812, 2021, doi: 10.22616/ERDev.2021.20.TF182.

[8] I. Lasenko *et al.*, "The Mechanical Properties of Nanocomposites Reinforced with PA6 Electrospun Nanofibers," *Polymers (Basel).*, vol. 15, no. 3, 2023, doi: 10.3390/polym15030673.

[9] K. K. Annamaneni, A. Korjakins, I. Lasenko, O. Kononova, A. Krasnikovs, and V. Lusis, "Experimental Study and Modelling on The Structural Response of Fiber Reinforced Concrete," *Multidiscip. Digit. Publ. Inst.*, 2022.

[10] S. Gaidukovs, I. Lyashenko, J. Rombovska, and G. Gaidukova, "Application of amber filler for production of novel polyamide composite fiber," *Text. Res. J.*, vol. 86, no. 20, pp. 2127–2139, 2016, doi: 10.1177/0040517515621130.

[11] J. V. Sanchaniya, I. Lasenko, S. P. Kanukuntla, A. Mannodi, A. Viluma-Gudmona, and V. Gobins, "Preparation and Characterization of Non-Crimping Laminated Textile Composites Reinforced with Electrospun Nanofibers," *Nanomaterials*, vol. 13, no. 13, 2023, doi: 10.3390/nano13131949.

[12] J. V. Sanchaniya *et al.*, "Mechanical and Thermal Characterization of Annealed Oriented PAN Nanofibers," *Polymers (Basel).*, vol. 15, no. 15, 2023, doi: 10.3390/polym15153287.

[13] D. Grauda *et al.*, "Establishment of Biotesting System to Study Features of Innovative Multifunctional Biotextile," *Proc. Latv. Acad. Sci. Sect. B Nat. Exact, Appl. Sci.*, vol. 77, no. 3–4, pp. 186–192, 2023, doi: 10.2478/prolas-2023-0026.

[14] A. Asar and W. Zaki, "A comprehensive review of the mechanisms and structure of interpenetrating phase composites with emphasis on metal-metal and polymer-metal variants," *Compos. Part B*, vol. 275, no. October 2023, p. 111314, 2024, doi: 10.1016/j.compositesb.2024.111314.

[15] E. A. Ananiadis, A. E. Karantzalis, A. K. Sfikas, E. Georgatis, and T. E. Matikas, "Aluminium Matrix Composites Reinforced with AlCrFeMnNi HEA Particulates: Microstructure, Mechanical and Corrosion Properties," *Materials (Basel).*, vol. 16, no. 15, 2023, doi: 10.3390/ma16155491.

[16] A. Shishkin, I. Hussainova, V. Kozlov, M. Lisnanskis, P. Leroy, and D. Lehmhus, "Metal-Coated Cenospheres Obtained via Magnetron Sputter Coating: A New Precursor for Syntactic Foams," *Jom*, vol. 70, no. 7, pp. 1319–1325, 2018, doi: 10.1007/s11837-018-2886-0.

[17] A. Shishkin *et al.*, "Cavitation-dispersion method for copper cementation from wastewater by iron powder," *Metals (Basel).*, vol. 8, no. 11, pp. 4–6, 2018, doi: 10.3390/met8110920.

[18] P. Colombo, "Cellular ceramics with hierarchical porosity from preceramic polymers," *IOP Conf. Ser. Mater. Sci. Eng.*, vol. 18, no. SPEC. SYMPOSIUM, 2011, doi: 10.1088/1757-899X/18/1/012002.

[19] V. Mironovs *et al.*, "Cellular structures from perforated metallic tape and its application for electromagnetic shielding solutions," *Agron. Res.*, vol. 12, p. (in Print), Jan. 2014.

[20] M. Pelanconi, D. Koch, G. Bianchi, S. Bottacin, and P. Colombo, "High-strength Si – SiC lattices prepared by powder bed fusion , infiltration-pyrolysis , and reactive silicon infiltration," no. December 2023, pp. 1–15, 2024, doi: 10.1111/jace.19750.

[21] V. Popov *et al.*, "Novel hybrid method to additively manufacture denser graphite structures using Binder Jetting," *Sci. Rep.*, vol. 11, no. 1, pp. 1–11, 2021, doi: 10.1038/s41598-021-81861-w.

[22] J. Baronins *et al.*, "The Effect of Zinc Oxide on DLP Hybrid Composite Manufacturability and Mechanical-Chemical Resistance," *Polymers (Basel).*, vol. 15, no. 24, 2023, doi: 10.3390/polym15244679.

[23] K. Irtiseva *et al.*, "Towards next-generation sustainable composites made of recycled rubber, cenospheres, and biobinder," *Polymers (Basel).*, vol. 13, no. 4, pp. 1–14, 2021, doi: 10.3390/polym13040574.

[24] A. Shishkin, V. Mironovs, V. Lapkovskis, J. Treijs, and A. Korjakins, "Ferromagnetic sorbents for collection and utilization of oil products," *Key Eng. Mater.*, vol. 604, pp. 122–125, 2014, doi: 10.4028/www.scientific.net/KEM.604.122.

[25] A. Shishkin, V. Mironov, D. Goljandin, and V. Lapkovsky, "Recycling of Al-W-B composite material," *Key Eng. Mater.*, vol. 527, pp. 143–147, 2012, doi: 10.4028/www.scientific.net/KEM.527.143.

[26] R. Ciardiello, L. T. Drzal, and G. Belingardi, "Effects of carbon black and graphene nano-platelet fillers on the mechanical properties of syntactic foam," *Compos. Struct.*, vol. 178, pp. 9–19, 2017, doi: 10.1016/j.compstruct.2017.07.057.

[27] V. Abramovskis *et al.*, "and Potential Applications," 2023.

[28] F. Hussain, M. Hojjati, M. Okamoto, and R. E. Gorga, "Review article: Polymer-matrix nanocomposites, processing, manufacturing, and application: An overview," *J. Compos. Mater.*, vol. 40, no. 17, pp. 1511–1575, 2006, doi: 10.1177/0021998306067321.

[29] S. Pavlidou and C. D. Papaspyrides, "A review on polymer-layered silicate nanocomposites," *Prog. Polym. Sci.*, vol. 33, no. 12, pp. 1119–1198, 2008, doi: 10.1016/j.progpolymsci.2008.07.008.

[30] D. S. More, M. J. Moloto, N. Moloto, and K. P. Matabola, "TOPO-capped silver selenide nanoparticles and their incorporation into polymer nanofibers using electrospinning technique," *Mater. Res. Bull.*, vol. 65, pp. 14–22, 2015, doi: 10.1016/j.materresbull.2015.01.030.

[31] L. Li, L. M. Bellan, H. G. Craighead, and M. W. Frey, "Formation and properties of nylon-6 and nylon-6/montmorillonite composite nanofibers," *Polymer (Guildf).*, vol. 47, no. 17, pp. 6208–6217, 2006, doi: 10.1016/j.polymer.2006.06.049.

[32] P. Tumiłowicz, L. Synoradzki, A. Sobiecka, J. Arct, K. Pytkowska, and S. Safarzynski, "Bioactivity of Baltic amber - Fossil resin," *Polimery*, vol. 61, pp. 347–356, May 2016, doi: 10.14314/polimery.2016.347.

[33] I. Lašenko, S. Gaidukovs, and J. Rombovska, "Manufacturing of amber particles suitable for composite fibre melt spinning," *Proc. Latv. Acad. Sci. Sect. B Nat. Exact, Appl. Sci.*, vol. 70, no. 2, pp. 51–57, 2016, doi: 10.1515/prolas-2016-0007.

[34] N. Wang, Y. Liu, Y. Liu, and Q. Wang, "A shear pan mill for preparation of ultrafine polyamide 66 powder using sodium sulfate ionic crystals as grinding aid," *Mater. Manuf. Process.*, vol. 32, no. 2, pp. 115–120, 2017, doi: 10.1080/10426914.2016.1221080.

[35] D. Chen, Q. Zeng, Y. Yuan, B. Cui, and W. Luo, "Baltic amber or Burmese amber: FTIR studies on amber artifacts of Eastern Han Dynasty unearthed from Nanyang," *Spectrochim. Acta - Part A Mol. Biomol. Spectrosc.*, vol. 222, p. 117270, 2019, doi: 10.1016/j.saa.2019.117270.

[36] A. A. Khomich, R. Khmelnitskii, M. Kozlova, A. V. Khomich, and V. Ralchenko, "IR Spectroscopy of Vacancy Clusters (Amber Centers) in CVD Diamonds Nanostructured by Fast Neutron Irradiation," *C-Journal Carbon Res.*, vol. 9, no. 2, 2023, doi: 10.3390/c9020055.

[37] H. Mahfuz *et al.*, "Reinforcement of nylon 6 with functionalized silica nanoparticles for enhanced tensile strength and modulus," *Nanotechnology*, vol. 19, no. 44, 2008, doi: 10.1088/0957-4484/19/44/445702.